

# Analysis of the Eccentricity Vector in Low Earth Orbits as Planar Rigid Body Motion

By Javier SANCHEZ,<sup>1)</sup> and Petr KUCHYNKA<sup>1)</sup>

<sup>1)</sup>GMV at ESA/ESOC, Darmstadt, Germany

(Received April 17th, 2017)

Eccentricity control in Low Earth Orbits is typically achieved by selecting the eccentricity vector close to the frozen eccentricity. In the vicinity of this stability point the long-periodic variations of the eccentricity vector are dominated by the Earth's Potential and the Solar Radiation Pressure perturbations. It has been proven that the combined effect of these two perturbations introduces an eccentricity vector variation analogous to the field of velocities of a rigid body in planar motion<sup>1)</sup>. This paper presents an innovative analysis of this interesting fact, where the known properties of this type of motion are applied to understanding the eccentricity behaviour and the design of control strategies. Planar rigid body motion is defined as the movement of a rigid body with respect to a fixed frame, where the free drift motion of the eccentricity vector can be represented as the trajectory of a point attached to the moving body, as seen from the fixed reference frame. Inherent properties of this type of motion, such as the preservation of distances within a rigid body, or the curves known as the moving and fixed centrodes for the Instant Centre of Rotation, have a direct application in the implementation of efficient eccentricity control techniques. Besides, the rigid body interpretation offers an elegant approach to the ever more challenging altitude control requirements of future missions. The work presented in this paper includes as well practical applications to the operational eccentricity control of real Earth observation spacecraft.

**Key Words:** Eccentricity Control, Frozen Eccentricity, Solar Radiation Pressure, Altitude Control

## Nomenclature

ICR : Instant Centre of Rotation  
LEO : Low Earth Orbit  
SRP : Solar Radiation Pressure

## 1. Introduction

Efficient eccentricity control is the key to achieve tight altitude control, which is of paramount importance in Earth observation missions. The study presented in this paper is focused on eccentricity control of low Earth orbits, controlled in the vicinity of the Frozen Eccentricity point, which is located at an argument of latitude close to 90 degrees. The results presented in the paper cover therefore a wide range of the orbits typically used for Earth observation missions. However, the study can also be expanded to other orbit types, such as geostationary missions, or orbits with similar dynamics in the motion of the eccentricity vector.

In LEO the eccentricity vector is primarily affected by the Earth's potential and the SRP perturbations. The Earth's potential perturbation alone leads to a stable circular motion of the eccentricity vector at constant angular velocity around the frozen eccentricity point.<sup>6) 7)</sup> On the other hand, the combined effect of these two perturbations induces an eccentricity vector change rate analogous to the field of velocities of a rigid body in planar motion.<sup>1)</sup> The dynamic model used to derive this result is a first order, analytical approximation of the effect of the Earth's potential and SRP forces using perturbations theory (Gauss planetary equations).

All other perturbations have been neglected. Although some of them may have a visible effect, the accuracy achieved by this dynamic model is sufficient to properly model the behaviour of the eccentricity vector. For instance, the oscillating effect due to the solid Earth tides is clearly visible (but not significant) when comparing the results of this dynamic model against full-force numerical propagations.

The study is focused on the long-periodic perturbations in the eccentricity vector. Thus, the effect of oscillations that take place along an orbit revolution, or fluctuations due to the differences in Earth's potential as the geodetic longitude of the equatorial nodes changes, are not considered in this study. Usually, the orbit control of Earth observation missions is implemented following a reference orbit, which includes these short-periodic variations. The comparison of the eccentricity vector against one such reference orbit reproduces the long-term behaviour that is tackled in this study. The graphical representation of these long-term variations in the eccentricity vector can be achieved in two ways:

1. Average eccentricity over a given time interval, usually an orbit repeat cycle. For orbits without a repeat cycle, accurate results can also be obtained by selecting averaging intervals finishing at similar longitudes.
2. Computation of the eccentricity vector with respect to a reference orbit, evaluated at equivalent geodetic locations (e.g. ascending node and same longitude).

The plots that are shown throughout this paper have been generated using the second method, that is by evaluating the eccentricity vector at the ascending node against the reference. Furthermore, the mean eccentricity vector of the reference orbits is assumed to be the frozen eccentricity point, that is, at the stability point for the eccentricity vector taking into account only the Earth's potential perturbation.

As shown in Ref. 1), the long-term behaviour of the eccentricity vector under the combined action of the Earth's potential and the SRP perturbation can be modelled as the differential equation shown in Eq. 1, where the eccentricity is expressed as a vector relative to the frozen eccentricity (Eq. 3). This is the equation, which describes the motion of the eccentricity vector. The term due to the contribution of the SRP (Eq. 4) is a function of the orbit characteristics (Semilatus Rectum, angular momentum), the length of the eclipses and SRP force, which is modelled using the cannonball SRP model.<sup>2)</sup> The derivative of the eccentricity vector given by Eq. 1 represents the field of velocities of a planar rigid body motion at constant angular velocity, since  $\vec{\Omega}$  is a constant vector. The angular velocity is a function at a larger scale of the semi-major axis and the orbit inclination.<sup>1) 6) 7)</sup> Alternatively, the eccentricity vector change rate can also be expressed as a function of its position with respect to the ICR (Eq. 2) by means of vector  $\vec{\rho}$  defined in Eq. 5, with the ICR position given by Eq. 6.

$$\dot{\vec{r}} = \vec{\Omega} \times \vec{r} + \vec{v}_{SRP} \quad (1)$$

$$\dot{\vec{r}} = \vec{\Omega} \times \vec{\rho} \quad (2)$$

where:

$$\vec{r} = \vec{e} - \vec{e}_{FE} \quad (3)$$

$$\vec{v}_{SRP} = \vec{v}_{SRP}(orbit, \Delta\theta, \vec{y}_{SRP}, \dots) \quad (4)$$

$$\vec{\rho} = \vec{r} - \vec{r}_{ICR} \quad (5)$$

$$\vec{r}_{ICR} = \frac{\vec{\Omega} \times \vec{v}_{SRP}}{\Omega^2} \quad (6)$$

If the position of the eccentricity vector with respect to the frozen eccentricity (Eq. 3) is large compared against the position of the ICR (Eq. 6) (e.g. eccentricity control carried out far away from the frozen eccentricity or  $\vec{r}_{ICR}$  small due to a small value of the SRP force) then the motion of the eccentricity vector approximates that of a pure rotation around the frozen eccentricity, as in the case when the Earth's potential perturbation alone is considered. The cases of interest are those where  $\vec{r}$  and  $\vec{r}_{ICR}$  are comparable in size, as shown in Eq. 7.

$$|\vec{r}| \sim \frac{|\vec{v}_{SRP}|}{\Omega} \quad (7)$$

During the preparation of this study, Ref 3) has been used as main reference for classic mechanics, in particular for the area of planar rigid body motion. However, the available literature on this topic is quite ample, see for example Ref 4)

and Ref 5).

## 2. Planar rigid body motion

Planar rigid body motion is defined as the motion of a moving rigid body with respect to a fixed reference frame. The motion takes place within a plane, that is, all velocities are parallel to a given reference plane and the angular velocity vector of the moving body is always orthogonal to that reference plane.

Due to the intrinsic properties of a rigid body, such as the non-deformation of points contained in the rigid body, the motion can be described as that of a moving reference frame with respect to a fixed one. Therefore, the terms moving and fixed body and moving and fixed frame shall be used interchangeably.

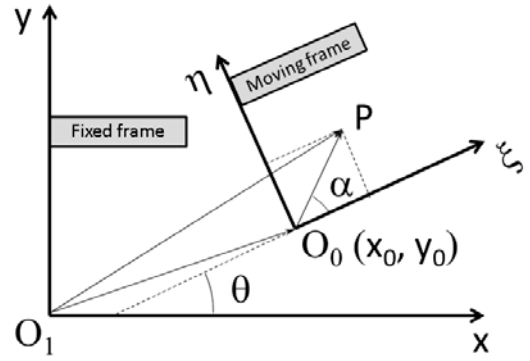


Fig 1. Definition of the fixed and moving frames.

$$x = x_0 + \xi \cos\theta - \eta \sin\theta \quad (8)$$

$$y = y_0 + \xi \sin\theta + \eta \cos\theta \quad (9)$$

Eq. 8 and 9 provide the transformation function between points in the fixed frame (x, y) and points in the moving frame ( $\xi, \eta$ ), as it can be deduced from Fig. 1. The fixed frame can be chosen to coincide with the ( $e_x, e_y$ ) reference frame, with the x axis pointing in the direction of the line of nodes and the y axis perpendicular to the previous one and contained within the orbital plane. The advantage presented by this frame is that, given a change in the eccentricity vector due to an orbit control manoeuvre in the velocity direction  $\vec{\Delta e}$ , the argument of latitude at which the manoeuvre took place can be directly measured as the angles from the x axis. In the moving frame this is not trivial and angles are linked by means of Eq. 10 where  $\varphi$  represents the argument of latitude and the rest of the angles as defined in Fig. 1. However, the transformation function for angles from the moving to the fixed frame is relatively simple due to the constant angular velocity of the motion.

$$\varphi = \alpha + \theta = \alpha + \Omega t - \theta_0 \quad (10)$$

The motion of the eccentricity vector can be understood as the trajectory followed in the fixed frame of a point attached to the moving frame. If the spacecraft eccentricity vector is unchanged (i.e. in free drift) the motion described by the eccentricity vector can be represented by just one single point in the moving frame. Should the spacecraft undergo an eccentricity change (e.g. an orbit control manoeuvre) the point representing the eccentricity motion changes to another one in the moving frame, and the trajectory described by the eccentricity vector, as seen from the fixed frame, also changes to a different one. Figure 2 illustrates the duality between points in the moving frame and curves described by the eccentricity vector in the fixed frame. Given an initial position for the eccentricity vector at  $t=t_0$ , represented by point  $P$  in the moving frame, the eccentricity vector describes a trajectory in the fixed frame represented by curve  $p$ . At  $t=t_1$  an eccentricity manoeuvre is executed changing the eccentricity vector to point  $Q$  in the moving frame, as a consequence of that the motion of the eccentricity vector in the fixed frame is changed to a different trajectory,  $q$ . At  $t=t_2$  a second eccentricity manoeuvre is executed, which sets the eccentricity vector back to the original  $P$  point in the moving frame. This allows returning to the original  $p$  curve in the fixed frame at a later stage.

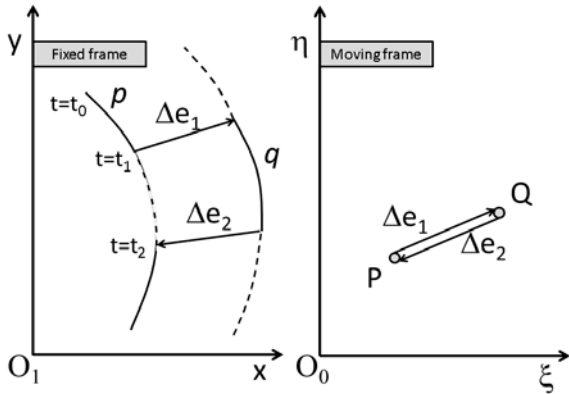


Fig 2. Duality between points and trajectories in the moving and fixed frames.

Perhaps the most evident property of rigid body motion is the preservation of distances within a rigid body, consequence of the non-deformation of a rigid body. Given a number of different points attached to the moving frame, each one representing the free drift eccentricity motion of the *same* spacecraft, the relative positions between them are preserved. The eccentricity vector evolution of each of these spacecraft follows a different trajectory, as seen from the fixed frame. However, since their trajectories are the consequence of the movement of the moving body with respect to the fixed frame, their relative distances (not the directions) are preserved at any given time. The spacecraft do not necessary need to be the

same, as long as they share the same characteristics from the dynamic point of view of this problem: same orbit (semi-major axis, inclination, local time) and the SRP perturbation is the same (same SRP coefficient, same reference surface, etc.). Figure 3 illustrates this fact by depicting the eccentricity vector evolution resulting from three different full-force model propagations with different initial conditions on their eccentricity vectors. This characteristic is useful when planning the eccentricity control of Earth observation constellations. Given a constellation of  $N$  spacecraft, following the same ground track, with a delay in the overflight of a given geographical area  $dt_i$  ( $i=1, \dots, N-1$ ), the altitude difference at which observations are taken by each one of the spacecraft can be minimized by selecting eccentricity vector offsets between them appropriately, such that their eccentricity vector is as close as possible to that of the other spacecraft when they overfly the geographical area in question.

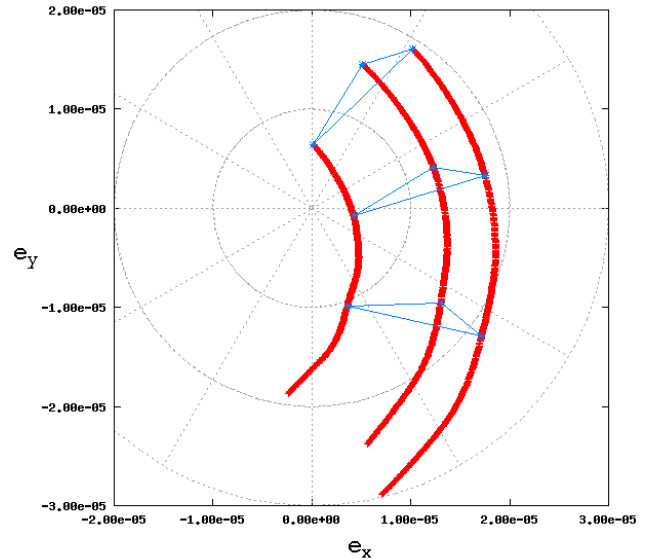


Fig 3. Preservation of distances between eccentricity vectors. Full-force propagation.

### 3. Fixed and moving centrodes

One of the characteristics of planar rigid body motion is the existence of an Instant Centre of Rotation. At any given time the motion of the moving frame can be expressed as a pure rotation around this point.<sup>3)4)5)</sup> The ICR is a free point in the motion, i.e. it is not attached to neither the fixed nor the moving frame. An observer in each one of the frames will see a different trajectory described by the ICR. The loci of positions occupied by the ICR in the fixed and moving frames receive the names of fixed and moving centrodes respectively. At all times, both centrodes are tangent to each other at the position of the ICR, and the field of velocities of the motion is originated by the rolling without sliding of the moving centrode on the fixed centrode. These two curves completely determine a given planar rigid body motion.<sup>3)</sup>

The representation of the fixed and moving centrodes is of paramount importance in the design of the eccentricity control strategy of a mission. The curve can be obtained in the fixed frame by finding the point of zero velocity (ICR position<sup>1)</sup>) as a function of time, by solving Eq. 1 equal to zero. Defining a reference point in the moving frame and knowing its trajectory in the fixed frame ( $x_0, y_0$ ), the moving centrodre can be computed via the transformation function given by Eq. 8 and 9.

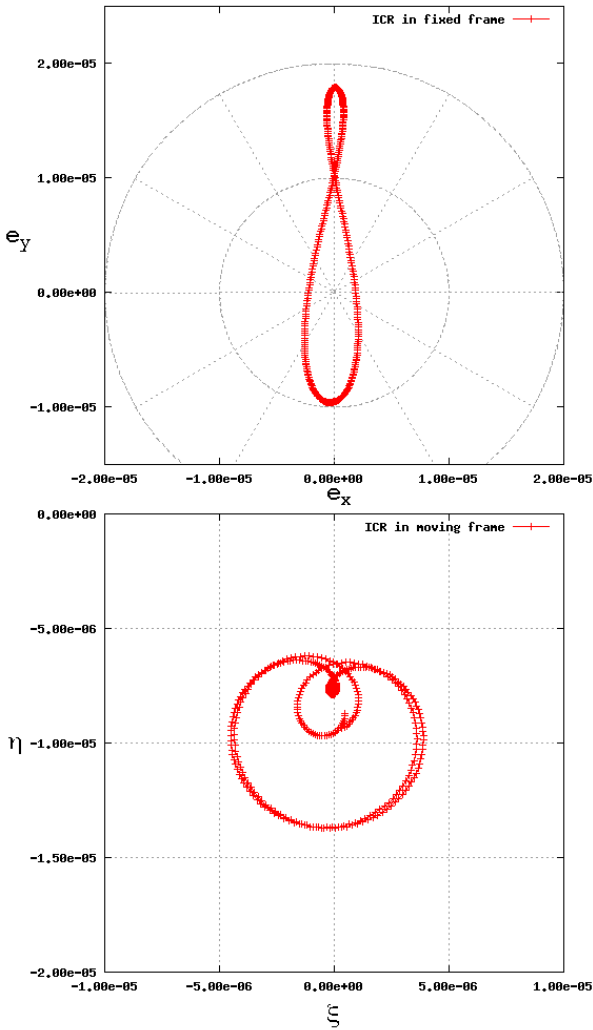


Fig 4. Fixed and moving centrodes for a sun-synchronous spacecraft with local time of descending node at 6:00 (Sentinel-1). Time span represented: 1 year.

Figure 4 and 5 provide the representation of the fixed and moving centrodes for two different sun-synchronous spacecraft. Namely a dawn-dusk orbit (Sentinel-1), and an orbit with a local time of descending node at 10:30 (Sentinel-2). The fixed centrodes of these two orbits are not symmetric with respect to the x axis, but slightly more elongated in the upper part, since both orbit inclinations are close to 98 degrees. The 10:30 local time of descending node

orientation can be noticed in the shift of the fixed centrodre of Fig. 5 towards the negative values of the x axis. The position of the moving centrodes within the moving plane is arbitrary and depends on the selection of a reference point and the initial orientation of the plane. Both fixed centrodes in Fig. 4 and 5 start and finish at the same point after a time span of one year. This occurs due to the SRP force having the same magnitude and direction with respect to the orbital plane after one year. After the same time span, the moving centrodre returns almost to the same starting point, this leads to a quasi-periodic motion of the eccentricity.

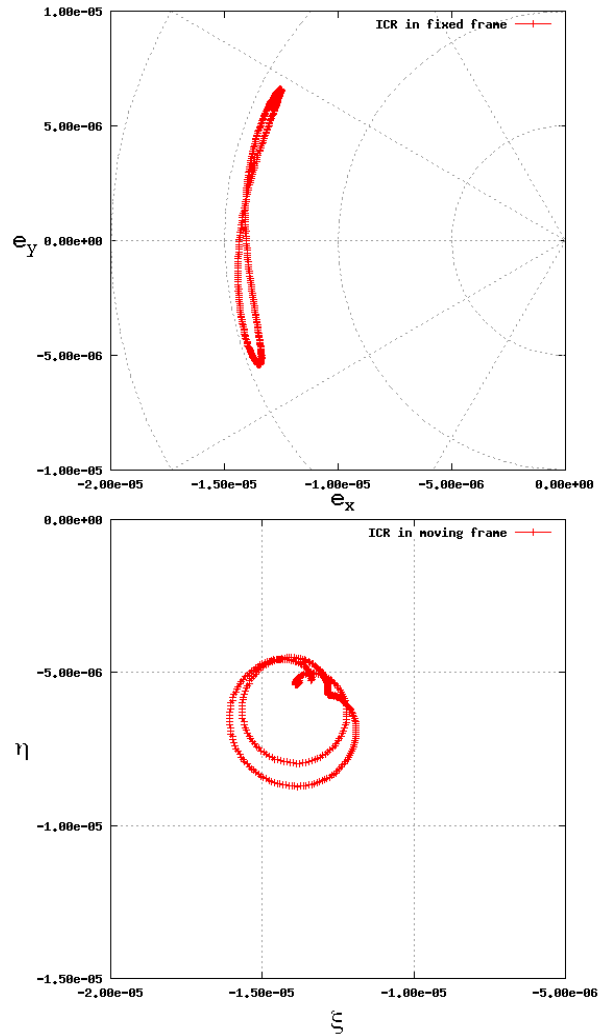


Fig 5. Fixed and moving centrodes for a sun-synchronous spacecraft with local time of descending node at 10:30 (Sentinel-2). Time span represented: 1 year.

Figure 6 depicts the fixed and moving centrodes of a non-sun-synchronous spacecraft in a polar orbit (CryoSat-2). Contrary to what happens in the case of a sun-synchronous spacecraft the fixed centrodre does not close after a given time span. This is due to the fact that the apparent motion of the sun with respect to the equator, 1 year period and amplitude given by the obliquity of the ecliptic, is not synchronized with

the motion of the line of nodes, which takes in this case approximately 483 days to complete a revolution in local time. Therefore, after 1 year, the Sun is in a different geometry leading to a different value for  $\vec{v}_{SRP}$ .

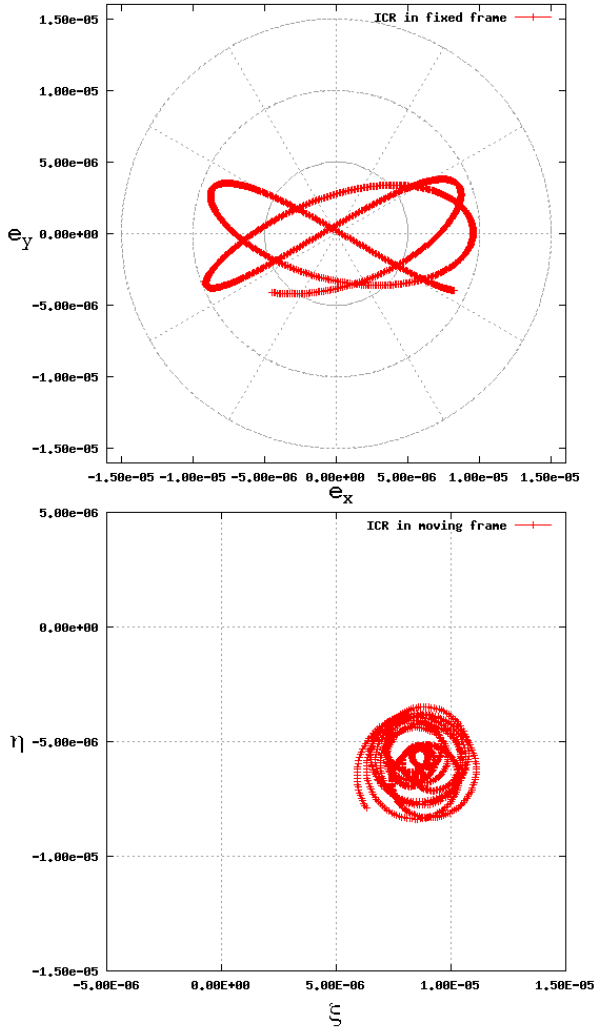


Fig 6. Fixed and moving centrodres for a non-sun-synchronous polar spacecraft (CryoSat-2). Time span represented: 3 years.

#### 4. Configurations for convergence and divergence of the eccentricity vector

As already introduced in the previous section the fixed and moving centrodres determine completely a planar rigid body motion. The different scenarios that can be faced regarding eccentricity control are many, depending on the orbit, SRP force and of course the requirements of each particular mission. However, there are some general conclusions that can be drawn from the motion of the eccentricity vector. In many cases the objective shall be to keep the eccentricity deviation as small as possible, or within predefined bounds, with respect to a reference. This endorses the study of the

monotonicity of the function describing the norm of the eccentricity vector, and the assessment in general terms of configurations that favour the convergence to (or the divergence from) the reference eccentricity.

$$\vec{u}_r \cdot \dot{\vec{r}} = \vec{u}_r \cdot (\vec{\Omega} \times \vec{\rho}) = \vec{\Omega} \cdot [\vec{u}_r \times (\vec{r}_{ICR} - \vec{r})] \quad (11)$$

where:

$$\vec{u}_r = \frac{\vec{r}}{r} \quad (12)$$

$$\dot{r} = \vec{\Omega} \cdot (\vec{u}_r \times \vec{r}_{ICR}) \quad (13)$$

As shown in Eq. 11, multiplying both sides of Eq. 2 by a unitary vector in the radial direction (Eq. 12) leads to the result expressed in Eq. 13. Since the angular velocity is a constant vector, the monotonicity of  $r$  depends on the cross product at the right hand side of Eq. 13. It can be inferred that the maximum values for the derivative of  $r$  are reached with a phase difference of 90 degrees between the unitary vector in the direction of the eccentricity vector and the ICR position. The ICR position depends on the orbit characteristics and the magnitude of the SRP force on the spacecraft. Therefore, for a given orbit and spacecraft this parameter cannot be influenced. The position of the eccentricity vector can be changed via orbit control manoeuvres. However, these manoeuvres are in general rather small, so that in most of the cases it will not be possible to relocate the eccentricity vector at any given phase with respect to the ICR.

An example of this behaviour can be seen in the free drift of the eccentricity vector in an orbit like the one proposed for the NASA/CNES mission SWOT. The orbit characteristics of this spacecraft are namely 890 km of altitude and a 77.6 degrees inclination of the orbital plane. The variable local time of this orbit leads to a fixed centrodre with a high circulation around the frozen eccentricity. Besides, this local time drift is in magnitude very similar to the angular velocity of the moving frame:  $\Omega$ . This means that if at a given epoch  $\vec{u}_r$  and  $\vec{r}_{ICR}$  are at a phase close to 90 degrees with respect to each other this configuration is kept for a long time period. As it can be seen in Fig 7 the evolution of the eccentricity vector starting from the frozen eccentricity leads to a divergence from this point. An eccentricity control law for this kind of orbit aiming at steering the eccentricity vector to the reference can be in some scenarios not the most adequate strategy. A possible solution to this problem could be to control the eccentricity vector following a circumference, and aiming orbit control manoeuvres not only at reducing  $r$ , but also at controlling the phase with respect to the ICR.

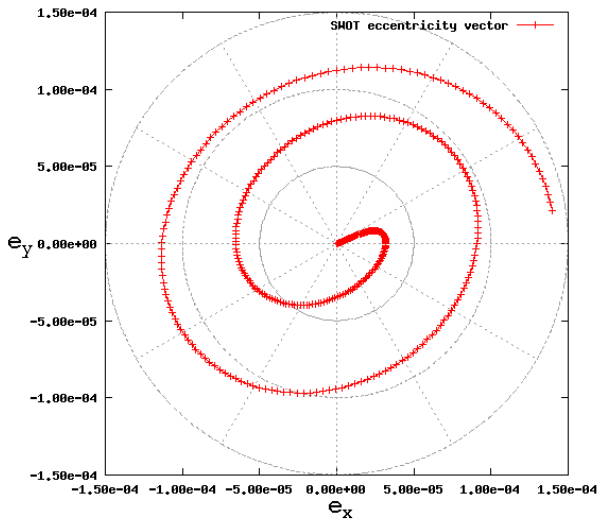


Fig 7. Evolution of the eccentricity vector in a SWOT-like orbit.

## 5. Application to the inter-solstice eccentricity control of Sentinel-1. The $\gamma$ trajectory

Ref. 1) provides an outline of the eccentricity control strategy implemented for the Sentinel-1 mission. The fixed centre of Sentinel-1 is similar to the one depicted in Fig. 6. During the summer and winter solstices the ICR is located at the top and bottom of the fixed centre respectively. The time span in which the ICR is close to the summer solstice position is relatively long: 3 months, whereas the ICR stays close to the winter solstice position for about 1 month. This implies that the motion of the ICR is relatively slow for the time periods close to the solstices. On the other hand, during the transition period between solstices the ICR moves rapidly towards the position at the next solstice. The time that it takes to the ICR to translate from the top to the bottom (and vice versa) of the fixed centre is approximately 4 months.

The eccentricity control requirements for Sentinel-1 are strict: the eccentricity vector has to be controlled inside a threshold of  $8.4E-6$  units of radius (blue circumference in Fig. 8), which is equivalent to maintaining the altitude deviations due to eccentricity error lower than 60 metres with respect to the reference orbit. During the summer solstice the ICR is located outside this threshold. As a consequence of this, the eccentricity control during the summer solstice is performed close to the upper end of the control area in order to avoid a fast eccentricity vector drift.<sup>1)</sup> In September the ICR enters the control area on its way towards the bottom of the fixed centre. The objective for the eccentricity control is to find a suitable point to set the eccentricity vector in order to follow the ICR on its way to the bottom of the fixed centre. If the objective is to move naturally downwards, together with the ICR, notice that setting the eccentricity vector exactly at the ICR position is not a good strategy, since the ICR is a zero

velocity point. The incentive to find a satisfactory solution to this problem is the existence in planar rigid body motion of a *point of equipollent velocity*<sup>3)</sup>: at any given time there is a point of the moving rigid body with the same velocity as the ICR translation velocity.

Eq. 1 and 2 have been integrated numerically in order to find initial conditions for a trajectory solution suitable for the transition period between solstices. The solution has been called  $\gamma$ -trajectory, named after the shape described by the eccentricity vector as seen from the fixed frame. The  $\gamma$ -trajectory is acquired in September at the top right of the eccentricity control area, close to the area where the eccentricity control is performed during the summer period. Once acquired, the eccentricity vector moves naturally towards the bottom of the eccentricity control area and returns automatically in April to the top left of the control area, where the summer solstice control of the following season can be started. In Figure 8 the eccentricity control carried out operationally for the Sentinel-1 mission has been depicted for the period September 2016 till April 2017, following the  $\gamma$ -trajectory. Small eccentricity corrections need to be done in order to compensate for: weekly in-plane orbit control manoeuvres, in-plane components of out-of-plane orbit control manoeuvres, collision avoidance manoeuvres (notice the effect of a collision avoidance manoeuvre in the large, one-time deviation from the nominal trajectory at the bottom of Fig 8), imperfections in the SRP modelling and higher order effects in the eccentricity motion. However, the  $\gamma$ -trajectory enables an almost effortless eccentricity control during the period between one summer solstice and the next.

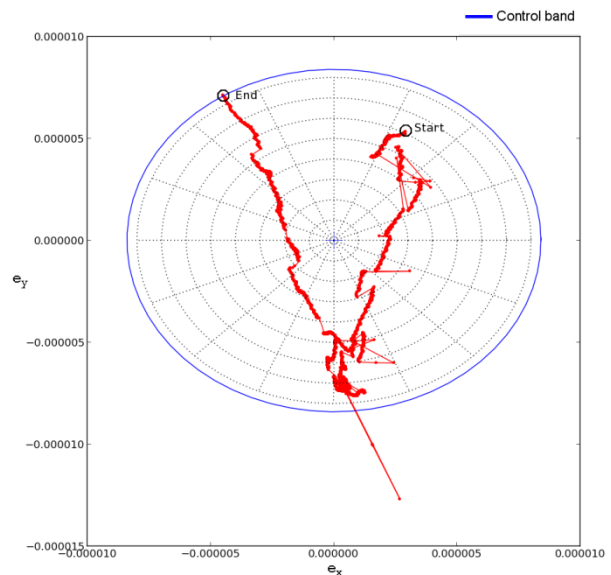


Fig 8. Sentinel-1 eccentricity vector following the  $\gamma$ -trajectory for the time period from September 2016 till April 2017.

## 6. Conclusion

Understanding the behaviour of the eccentricity vector under the effect of its main perturbing forces, the Earth's potential and the SRP, is fundamental for the development of efficient eccentricity control strategies in LEO missions. It allows the reduction of costs associated to the eccentricity correction, but also enables the compliance of even more challenging eccentricity control requirements.

The work presented in this paper introduced known elements of planar rigid body kinematics, which are of direct application to the eccentricity control of LEO spacecraft. The behaviour of the eccentricity vector has been studied for a wide range of LEO missions, and the examples presented are considered to be representative of the ideas intended to be transmitted. The approach presented in this paper can be taken as a recommendation for the analysis of the eccentricity control of other spacecraft, emphasizing the importance of studying the motion in both, the fixed and the moving frame, as well as the representation of the fixed and moving centrodes in the design of eccentricity control strategies for LEO spacecraft.

## Acknowledgments

I would like to thank the whole Flight Dynamics Earth Observation team at ESOC for their support and valuable contribution to this study.

## References

- 1) Sánchez, J., Martín Serrano, M. A. and Mackenzie R.: Characterization of the Solar Radiation Pressure Perturbation in the Eccentricity Vector, Proceedings 25<sup>th</sup> International Symposium on Space Flight Dynamics – 25<sup>th</sup> ISSFD. Munich, Germany, 2015.
- 2) Dennis D. McCarthy (ed.): IERS Standards (1989), (IERS Technical Note ; 3), Chapter 14: Radiation Pressure Reflectance Model, Paris: Central Bureau of IERS - Observatoire de Paris, 1989. iv, 77 p.
- 3) Prieto Alberca, M.: Curso de Mecánica Racional, Madrid 1986, ISBN 398-7697-1.
- 4) Simón Mata, A. et al.: Fundamentals of Machine Theory and Mechanisms, Springer 2016, ISBN 978-3-319-31970-4.
- 5) Homer D. Eckhardt,: Kinematic Design of Machines and Mechanisms, McGraw Hill Professional, 1998, ISBN: 978-0070189539.
- 6) D. A. Vallado: Fundamentals of Astrodynamics and Applications, Space Tegnology Library. Springer (2007) , ISBN 0-7923-6903-3.
- 7) Rosengren, M.: Improved Technique for Pasive Eccentricity Control, American Astronautical Society Publication, AAS-89-155 1989.